

Compressive Deformation Behaviour of Superplastic Y-TZP-Based Ceramics: Role of Grain Boundary Phases

J. L. Shi, G. Q. Zhu & T. R. Lai

Shanghai Institute of Ceramics, 1295 Ding-xi Road, Shanghai 200050, People's Republic of China

(Received 22 March 1996; revised version received 30 June 1996; accepted 15 July 1996)

Abstract

The compressive deformation behaviour of Y-TZP-based ceramics was investigated for its dependence on temperature, applied stress, grain size and the grain boundary phases of the materials. The deformation behaviour of the materials depends strongly on the grain boundary phase and the testing temperature. At 1250°C and above, the presence of LAS glass at boundaries in Y-TZP leads to much promoted deformation rates; while at temperatures lower than 1250°C, the LAS added composites show apparent retarded deformation. The activation energy for the compressive deformation was calculated to increase from 410 kJ/mol for pure Y-TZP to 784 kJ/mol for the composite with 5 vol% LAS glass addition from 1150 to 1350°C. Strain hardening effect is limited for testing at 100°C below sintering temperatures, and the grains retained their equiaxed shape after deformation. The deformation of Y-TZP/Al₂O₃ composite shows a mixed effect of alumina particles and the very small amount of glass phase at triple points in the bulk. Some small cavities were found at triple points for single-phase Y-TZP but no cavities can be identified in the materials containing some glass phase. The mechanism of the superplastic flow of the material is believed to be grain boundary sliding. © 1997 Elsevier Science Limited. All rights reserved.

1 Introduction

Y-TZP ceramics were first found by Wakai^{1–3} to show superplasticity at high temperatures. Later research work on the superplastic flow behaviour of the materials has been extensively reported, and several reviews on the superplasticity can be found.^{4–6} The superplasticity⁷ of a material is a type of uniform deformation ability without fracture, with the diffusion creep accommodated by

boundary sliding as the main mechanism; therefore, the grains remain equiaxed during deformation. A tensile deformation test is usually demanded for superplasticity research. However, for the purpose of the application of superplasticity for the near-net shaping of a sintered material, tensile deformation is prone to cause degradation of the performance of the deformed materials because of microstructural change such as cavitation and grain growth,¹ so for the real use of superplasticity, compressive deformation^{2,8–10} will probably be used more extensively and reliably. Other advantages of compressive deformation are, first, compressive testing is much easier than tensile testing, and, second, the deformed material can be tested for microhardness and micro-indentation toughness without much difficulty.

Superplastic deformation of materials has been recognised as a boundary process, mainly boundary sliding, as the superplastically deformed material usually shows its original equiaxed grain shape after a large amount of deformation.⁷ In this term, the grain boundary phase will play an important role in deformation.¹¹ This paper presents the results of the compressive deformation behaviour of pure Y-TZP ceramics and alumina particle and glass phase doped Y-TZP composites, the mechanical behaviour of deformed materials will be reported in a following paper.¹² The bi-axial stretching of the Y-TZP and Y-TZP/Al₂O₃ composites is also to be reported.¹³

2 Experimental Procedures

2.1 Material preparation

Y-TZP ceramics were fabricated by pressureless sintering of superfine powders, which were prepared via a coprecipitation method.^{14,15} As the prepared powder is free from hard agglomerates

the materials can be sintered to near theoretical density ($\geq 98\%$ TD) at temperatures as low as 1350°C . The Y-TZP-based composites, alumina particles (AKP-50, Sumitomo Chemicals) or LAS glasses (Li_2O : 3.0 wt%, Al_2O_3 : 23 wt% and SiO_2 : 74 wt%, transient point: $1200\text{--}1220^\circ\text{C}$ by DTA) were added by ball milling with alumina balls as the milling media. The alumina content was designed to be from 5 to 40 vol%, and that for LAS glass is 2 and 5 vol%. To obtain materials with different grain sizes, the materials were sintered at different temperatures from 1350 to 1650°C for 120 min. Y-TZP/ Al_2O_3 composites were sintered at 1550°C and Y-TZP/LAS-glass composites were sintered at 1250 or 1350°C . The samples were cut and ground into $4 \times 4 \times 8$ mm cuboids for the compressive tests.

2.2 Compressive deformation tests

Unlike the loading method reported by others,^{2,8,9} where deformation was performed at fixed cross-head speed, in the present study the cuboid specimens were loaded with a constant load along the longer axis after temperatures were raised and stabilised while the strain rate and the stress were functions of the deformation process. The dead loads were decided according to the applied stress desired and the arm ratio of the loading beam. The upper movable loading head was strictly guided to prevent eccentric loading. The specimens were placed in the middle of the hot zone which is considerably longer than the specimens. Two silicon carbide platens were used at the two ends of the specimens as the loading platens and no reaction or sticking was found between the specimens and silicon carbide after testing. Alumina rods were used for the load transfer between the hot zone and the cooled loading heads which were outside the furnace. The deformation displacements were measured with a mechanical LVDT and the signal was transferred into digital data and recorded with a computer. The deformation tests were generally performed for 5 h except where noted.

2.3 Strain and stress analysis

The strains of the deformed specimens were calculated according to the area change of the cross-section normal to the loading direction; strain rate is the area change divided by true cross-section area in the process in unit time period and the true stress during deformation was calculated following the increase of cross-section area:

$$\varepsilon (\%) = (A - A_0)/A_0 \quad (1)$$

$$\dot{\varepsilon} (\text{min}^{-1}) = (A_2 - A_1)/A_1/\Delta t \quad (2)$$

$$\sigma (\text{MPa}) = \sigma_0/(\varepsilon + 1) \quad (3)$$

where ε and $\dot{\varepsilon}$ are the nominal strain and the true strain rate, A_0 , A are the cross-sectional areas before and during deformation, A_2 and A_1 are the cross-sectional areas at two closest time points: t_1 and t_2 , $\Delta t = t_2 - t_1$; σ and σ_0 are the true applied stress during and before deformation. Because of the friction between the specimens and silicon carbide during deformation, the specimens were no longer real cuboids during deformation, and the stresses in the specimens were not uniform. Therefore the stress calculated in eqn (3) is only an averaged stress value.

2.4 Microstructure analysis

Microstructures of undeformed and deformed specimens were analysed with SEM on polished and thermally etched surfaces and TEM on the ion-thinned foils.

3 Results

3.1 Temperature dependence of the deformation behaviour

Figures 1 and 2 show the strain versus time and strain rate versus strain plots of the 1550°C sintered sample deformed at different temperatures. It is obvious, as has been regularly observed, that at high temperatures high strain rates were activated and therefore larger strains were obtained in the limited time period.

3.2 Stress dependence

The stress dependence of the deformation behaviour of 1450°C sintered Y-TZP samples deformed at 1350°C under different initial applied stresses is shown in Figs 3 and 4. It is also clear, as expected, that enhancing the initial applied stress leads to increased strain and strain rate.

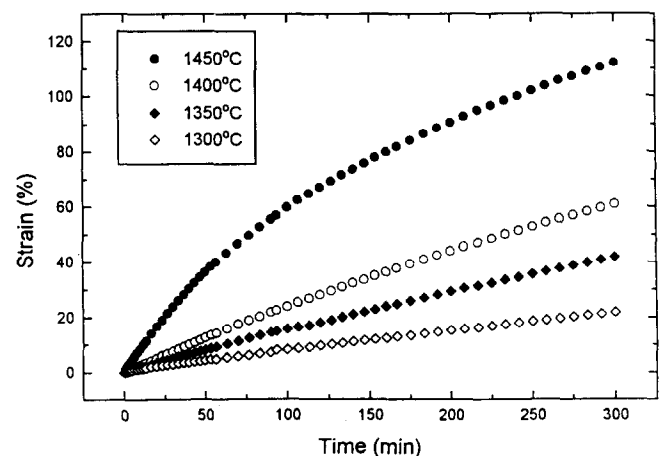


Fig. 1. Strain versus time plots of the 1550°C sintered specimens deformed at different temperatures and at the initial applied stress of 55 MPa.

3.3 Grain size dependence

Samples obtained by sintering at 1450, 1550 and 1650°C have different grain sizes. The grain sizes of the three specimens, calculated with the intersection method on the SEM photographs, are 0.32, 0.57 and 1.10 μm , respectively. The different

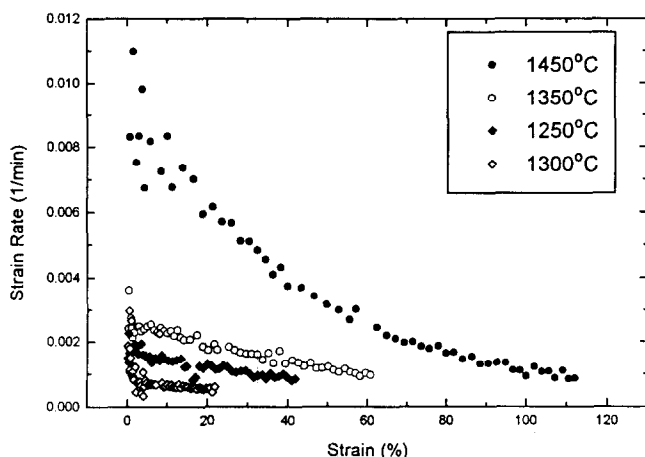


Fig. 2. Strain rate versus strain plots of the 1550°C sintered specimens deformed at different temperatures and at the initial applied stress of 55 MPa.

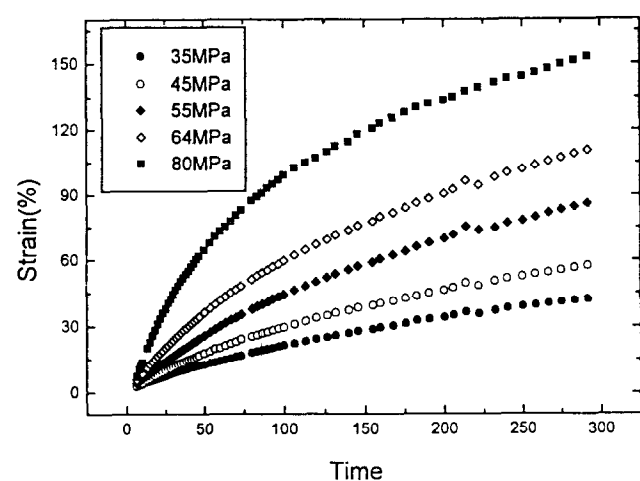


Fig. 3. Strain versus time plots of the 1450°C sintered specimens deformed at 1350°C and at different initial applied stresses as noted in the figure.

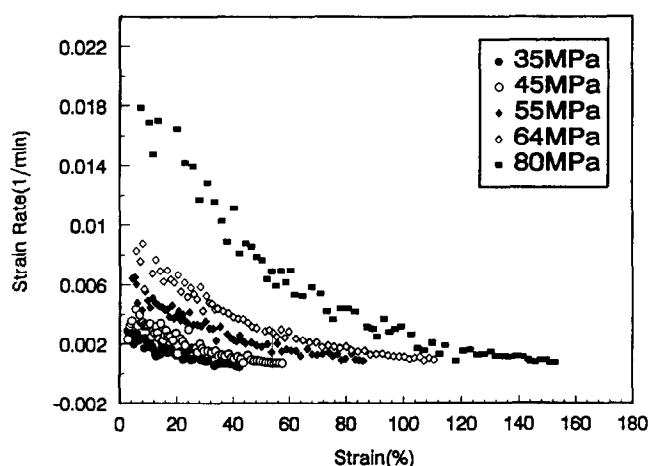


Fig. 4. Strain rate versus strain plots of the 1450°C sintered specimens deformed at 1350°C and at different initial applied stress.

grain sizes of the materials result in very different deformation behaviour, as can be seen in Figs 5 and 6 for the deformation at 1350°C. This behaviour reflects the role of the boundary density in the material on the deformation flow, as will be discussed in the next part.

3.4 Effect of grain boundary glass phase

Figure 7 gives the strain rate versus strain relations for 1350°C sintered Y-TZP/LAS-glass composites deformed at 1250°C. Such an effect of the glass phase on compressive deformation was also identified by Yoshizawa *et al.*¹¹ However, if the composite were deformed at lower temperature, the promoting effect of glass phase on the deformation will no longer exist, as can be found in Fig. 8 for 1350°C sintered composites deformed at 1050°C. Clearly, at 1050°C, the addition of LAS glass phase impedes the deformation of the materials. The detailed study shows that transition of the deformation behaviour of the composites with temperature is around 1150 to 1250°C.

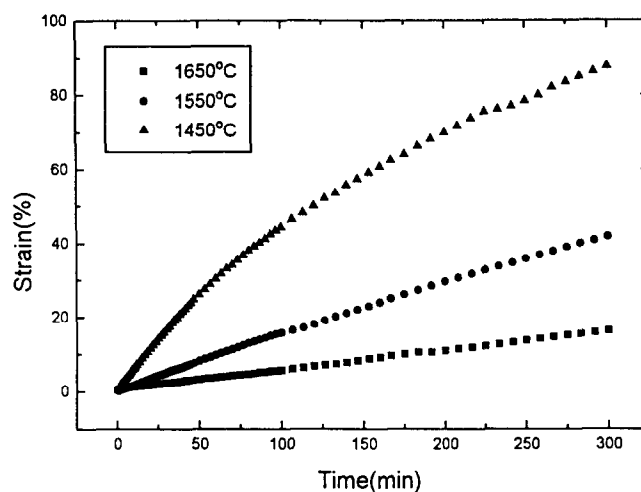


Fig. 5. Strain versus time plots for specimens sintered at different temperatures (as noted in the figure) and deformed at 1350°C with the initial applied stress of 55 MPa.

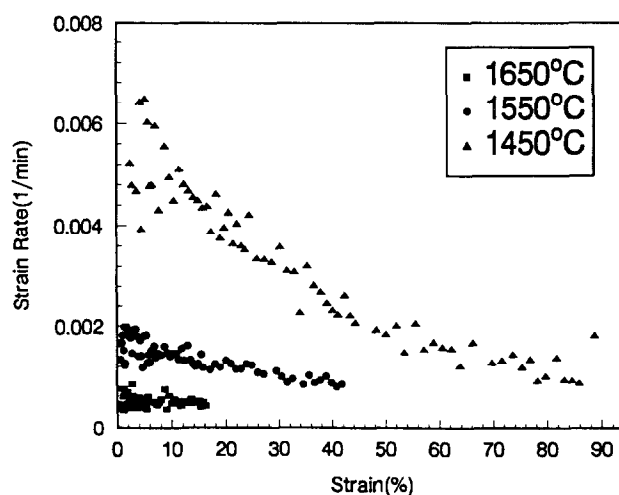


Fig. 6. Strain rate versus strain plots for specimens sintered at different temperatures (as noted in the figure) and deformed at 1350°C with the initial applied stress of 55 MPa.

From the $\ln(\text{strain rate})$ versus $1/T$ plots as shown in Fig. 9, which is obtained from the data at the beginning of deformation ($\epsilon \leq 5\%$) in the temperature range of 1050 to 1350°C, the activation energies were calculated to be 410, 535 and 784 kJ/mol for the composites containing 0, 2 and 5 vol% LAS glass, respectively. This shows that the activation energy of the deformation is not only a function of the glass composition,¹¹ but also a function of glass content.

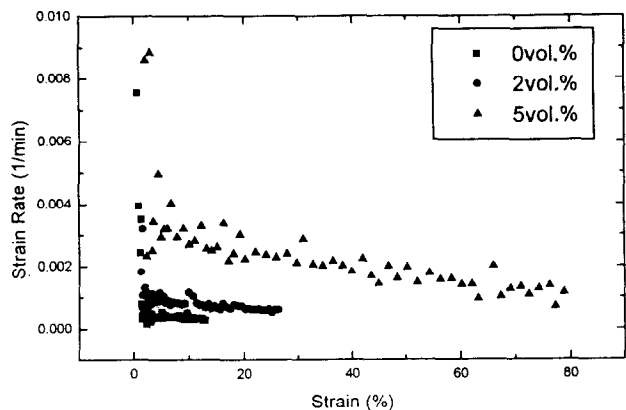


Fig. 7. Strain rate versus strain plots of the 1350°C sintered Y-TZP/LAS-glass composites deformed at 1250°C.

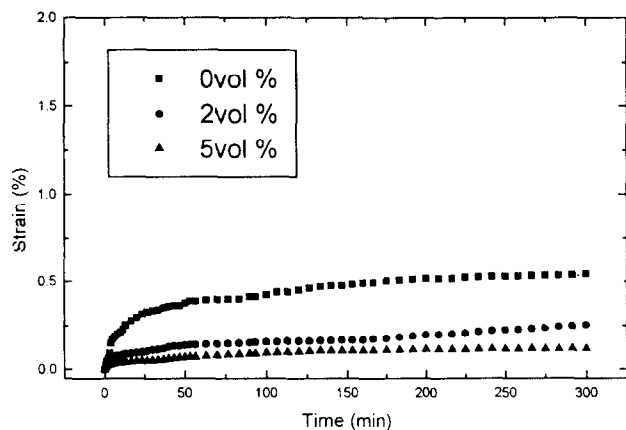


Fig. 8. Strain versus time plots of the 1350°C sintered Y-TZP/LAS-glass composites deformed at 1050°C.

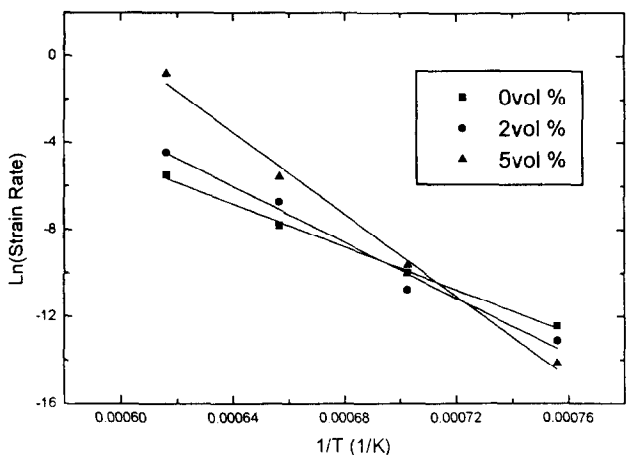


Fig. 9. Dependence of $\ln(\text{strain rate})$ on temperature for the Y-TZP/LAS-glass composites.

3.5 Effect of alumina particle addition

Figures 10 and 11 are the strain versus time and the strain rate versus strain profiles of the Y-TZP/ Al_2O_3 composite materials at 1450°C. The materials clearly become much easier to deform when alumina is added, leading to much larger strains and much higher strain rate of the materials, especially at low alumina content. As reported on the superplastic flow behaviour of the Y-TZP/ Al_2O_3 composites,^{16–18} the effect of alumina in the materials is to impede the materials' flow. This is simply because alumina has considerably higher Young's modulus than Y-TZP and thus alumina particles located at the boundaries will certainly pin the grain boundary sliding during deformation. The observed decreased deformation rate of the composites with increasing alumina content shows this effect. However, much enhanced deformation rate at only 5 and 10 vol%, as compared to the single phase Y-TZP, is believed to be caused by other reason(s), as will be discussed later by combining with microstructure analysis.

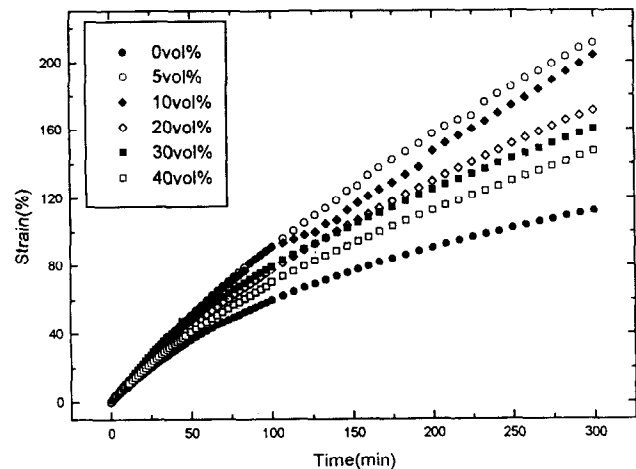


Fig. 10. Strain versus time plots of Y-TZP/ Al_2O_3 composites with different alumina content deformed at 1450°C and the initial applied stress of 55 MPa.

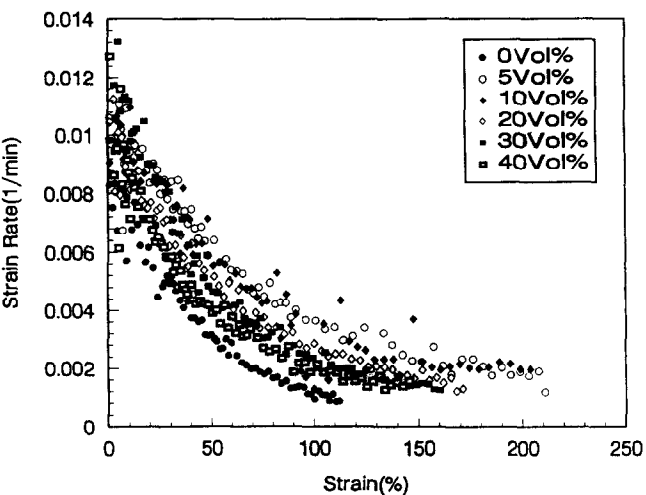


Fig. 11. Strain rate versus strain plots of the Y-TZP/ Al_2O_3 composites with different alumina content deformed at 1450°C and the initial applied stress of 55 MPa.

3.6 Microstructure change of the deformed materials

3.6.1 Single-phase Y-TZP

Reports^{1,19} have shown that strain-enhanced, or dynamic, grain growth, dependent on the deformation temperature, may occur in the deformation of superplastic Y-TZP. The compressively deformed materials at 100°C lower than the sintering temperature of 1450°C in the present study show very limited grain growth at the strain of 100%, as illustrated in Fig. 12. Cavitation in the SEM microstructure cannot be observed; however, small cavities can be found at some triple points

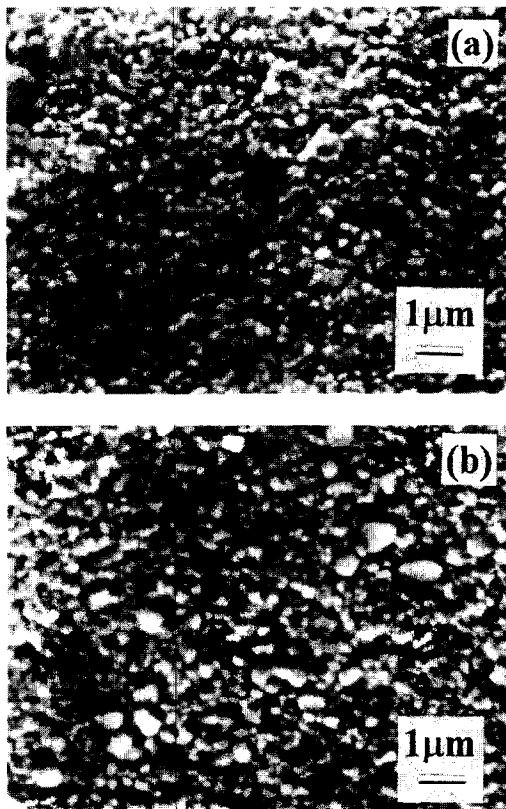


Fig. 12. SEM microstructures of 1450°C sintered specimens, (a) before deformation, (b) deformed at 1350°C to 100% strain.

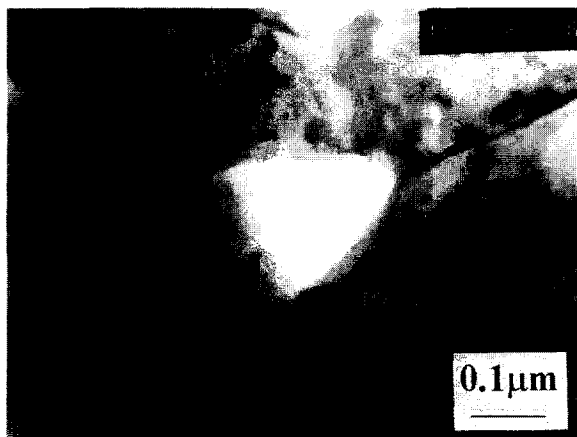


Fig. 13. A cavity at a triple point in the 1450°C deformed Y-TZP.

with TEM as shown in Fig. 13, but this phenomenon is not prevailing in compressively deformed materials. The tensile stress perpendicular to the loading axis is responsible for the very small cavities arising during deformation.

3.6.2 Y-TZP/LAS-glass composites

Similar to single-phase Y-TZP, the glass-phase-added composites experience negligible grain growth if deformed at about 100°C below the sintering temperature, as shown in Fig. 14 for the composites sintered at 1350°C and deformed at 1250°C.

3.6.3 Y-TZP/ Al_2O_3 composites

The deformed composites experience a considerable grain growth process, as can be found in Fig. 15 for the composite at 10 vol% alumina content. From the figure it can be clearly seen that the much enhanced grain growth of the deformed materials is mainly for Y-TZP grains; alumina grains mainly remain unchanged after deformation. Figure 16 shows evidence of a very small amount of glass phase present at the triple points, and after deformation, the glass 'points' were found to have accumulated with each other

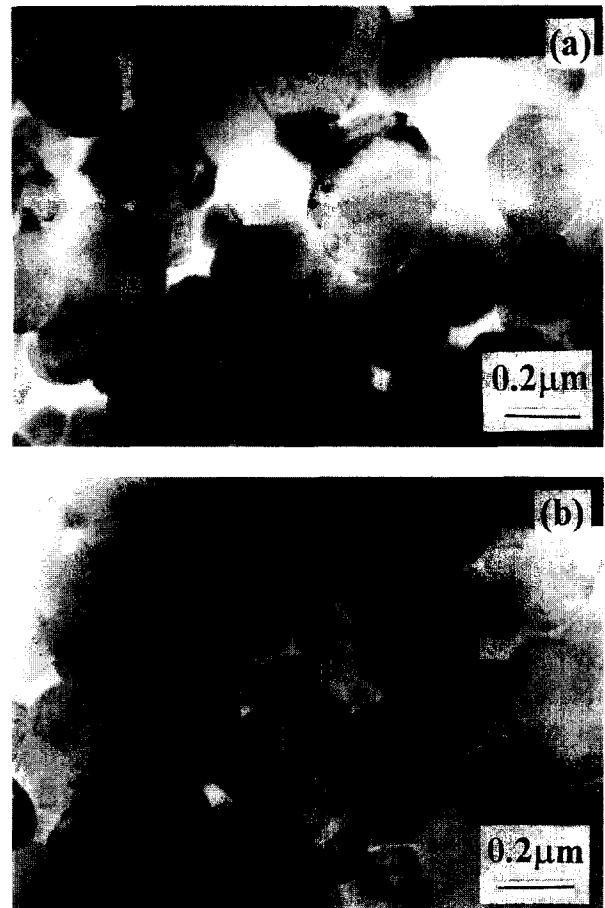


Fig. 14. TEM microstructure of the 1350°C sintered Y-TZP/5 vol% LAS-glass composites, (a) before deformation, (b) deformed at 1250°C to 80% strain.

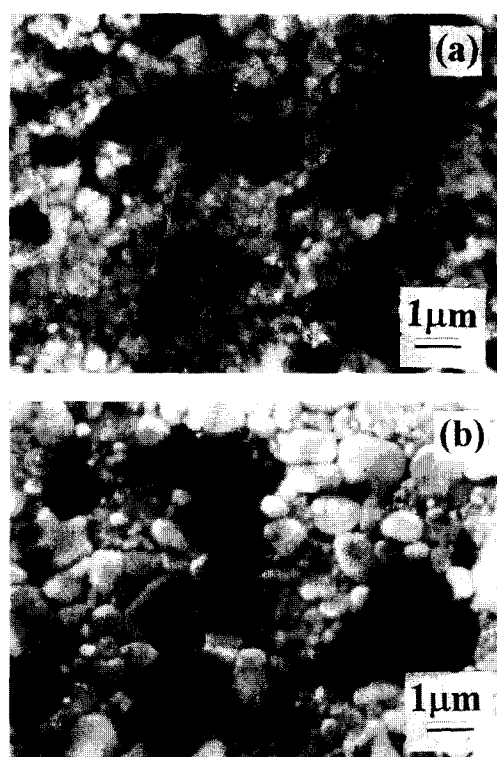


Fig. 15. SEM microstructures of the 1550°C sintered Y-TZP/10 vol% Al_2O_3 composites, (a) before deformation, (b) deformed at 1450°C to 200% strain.

accompanying grain growth. The detailed observation of microstructure and its effect on mechanical properties of the composites will be presented elsewhere.¹²

4 Discussions

4.1 Activation energy: effect of boundary glass phase

The measured activation energy of 410 kJ/mol for single-phase Y-TZP is in good agreement with that (380 kJ/mol) obtained by Wakai *et al.*² for the same material under similar deformation conditions as the material used by Wakai *et al.* is prepared from coprecipitated fine powders² which are the same as used in the present investigation. For the Y-TZP/LAS-glass composites, in the lower temperature range, the activation energy is glass-phase dependent, i.e. the presence of a small amount of glass phase at boundaries changes the deformation behaviour of the materials. This explains the scattering around the magnitude of the activation energy measured by different authors. The activation energy of 570 kJ/mol by Ducloux *et al.*⁹ can therefore be reasoned to be mainly related to some glass phase at boundaries and triple points.

4.2 Effect of alumina particles

The addition of alumina particles to the composites leads to enhanced deformation. However, there is still clear evidence for the impedance effect

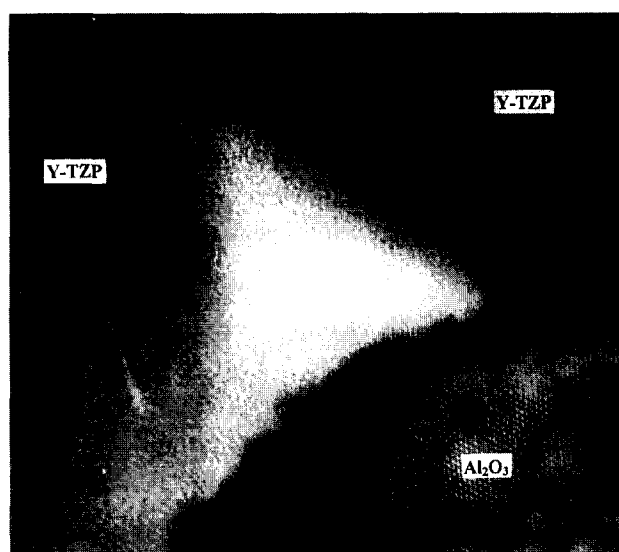


Fig. 16. HREM micromorphology of the Y-TZP/ Al_2O_3 composites containing 20 vol% alumina after deformation to 170% strain.

of alumina particles: with the increase of alumina content from 5 vol% to 40 vol%, the deformation rate of the composites was suppressed to some extent. This is easy to understand as the more rigid alumina particles in the materials will indeed impede the deformation of the TZP matrix. The presence of rigid alumina particles at the boundaries in the Y-TZP matrix will block the sliding between Y-TZP grains and therefore impede its deformation. The small amount of glass phase was believed to be introduced into the composites during mechanical mixing of Y-TZP and alumina via ball milling.

4.3 Effect of microstructure change on deformation

Since the strain-enhanced grain growth during deformation has been observed to be very limited in the present case, the strain-hardening effect, which is mainly due to the decrease of grain boundary densities, i.e. grain growth, in this study during the deformation is too slight to influence the deformation process of single-phase Y-TZP seriously.

The microstructure change of the Y-TZP/ Al_2O_3 composites, mainly the grain growth of Y-TZP, is significant at 1450°C. Pure single-phase Y-TZP shows only very limited grain growth at that temperature, and alumina particles themselves can only impede grain growth or have limited effect even at the sintering temperature of 1550°C,¹² so the significant grain growth is related to the applied stress and the presence of a small amount of glass phase in the microstructures.

The grain growth of the materials will impede their deformation, as found for single-phase Y-TZP where no boundary glass phase was present. However, for the Y-TZP/ Al_2O_3 composite

materials in this investigation, the situation was different. Grain growth not only results in the decrease of boundary density on the one hand, but also in the increase of the amount of glass phase at each triple point. These two factors may compensate for each other and thus the deformation behaviour of the composite may not be affected seriously by the microstructure change during deformation. Indeed, the smaller stress exponents and the smaller shape coefficients of the composite sample after deformation, than pure Y-TZP, do indicate that the glass phase must have promoted the superplastic flow via a boundary sliding process during deformation.

The cavitation in the compressive deformed 3Y-TZP was not found by Wakai *et al.*² because of the low-resolution SEM technique used. In the present study the cavitation phenomena were verified with TEM which possesses higher image resolution than SEM for pure Y-TZP without a glass phase. However, in the Y-TZP/LAS-glass and Y-TZP/Al₂O₃ composites, cavitation was not identified with TEM. This shows that the small amount of glass phase could fully accommodate the deformation led by a boundary sliding process,²⁰ and that the boundary sliding is the controlling process in the deformation. Unlike the present study, cavitation phenomena but with much larger cavity size, were also found by Duclous *et al.*⁹ for Y-TZP with a certain glass phase; this is probably due to the different kind of glass phase present in the materials of Duclous *et al.*

4.4 Superplastic deformation mechanism

As the grains in all kinds of materials remain equiaxed during deformation, the large amount of deformation here is also reasoned to be a boundary process, mainly boundary sliding. The small amount of glass phase at the boundary will affect the sliding process. At higher temperatures than the glass transition point, the glass phase acts as the lubricant for the sliding and provide the fast diffusion path to accommodate the sliding. However at lower temperature than the transition point, the rigid nature of the glass phase makes the boundary sliding more difficult than in the materials without it. The promoted deformation of the Y-TZP/Al₂O₃ composites is also believed to be caused by the very small amount of glass phase at the triple points, as can be seen in Fig. 16.

5 Conclusions

The compressive deformation studies of single-phase 3Y-TZP and materials based on it show that:

1. The temperature dependence of the superplastic strain rate is related to the glass phase at boundaries; a higher content of the boundary phase leads to higher value of the activation energy.
2. Deformation rate of the Y-TZP/LAS-glass composites was greatly enhanced at 1250°C or higher, but impeded at lower temperature like 1050°C. This is believed to be related to the transition of the glass phase.
3. Y-TZP/Al₂O₃ composites also show the greatly enhanced deformation at relatively high temperature (1450°C). This is caused by the presence of very small amounts of glass phase at triple points. The impedance effect of alumina particles on deformation, though masked by the effect of glass phase, can still be identified.
4. Limited grain growth and strain hardening during deformation for Y-TZP and Y-TZP/LAS-glass composites were found if deformed at 100°C below the sintering temperature. The pronounced growth of Y-TZP grains in Y-TZP/Al₂O₃ composites was identified.

References

1. Wakai, F., Sakaguchi, S. & Matsuno, Y., Superplasticity of yttria stabilized tetragonal ZrO₂ polycrystals. *Adv. Ceram. Mater.*, **1**[3] (1986) 259–263.
2. Wakai, F., Kodama, Y. & Nagano, T., Compressive deformation and microstructures in the superplastic Y-TZP. *J. Ceram. Soc. Jpn.*, **94**(8) (1986) 721–725.
3. Wakai, F., Kodama, Y. & Nagano, T., Superplasticity of ZrO₂ polycrystals. *Jpn J. Appl. Phys.*, **28** (1989) 69–79.
4. Chen, I-Wei & Xue, Liang An, Development of superplastic structural ceramics. *J. Am. Ceram. Soc.*, **73**(9) (1990) 2585–2609.
5. Maehara, Y. & Langdon, T., Review: Superplasticity in ceramics. *J. Mater. Sci.*, **25** (1990) 2275–2286.
6. Wakai, F., Superplasticity of ceramics. *Ceram. Intl*, **17** (1991) 153–169.
7. Poirier, J.-P., Diffusion creep, grain boundary sliding and superplasticity. In *Creep of Crystals*, Cambridge University Press, London and New York, 1985, pp. 194–212.
8. Carry, C. & Moccellini, A., Structural superplasticity in single-phase crystalline ceramics. *Ceram. Intl*, (1987) 89–98.
9. Duclous, R., Crampon, J. & Amana, B., Structural and topological study of superplasticity in zirconia polycrystals. *Acta Metall.*, **37**(3) (1989) 877–883.
10. Duclous, R. & Crampon, J., High temperature deformation of a fine grain-sized zirconia. *J. Mater. Sci. Lett.*, **6** (1987) 905.
11. Yoshizawa, Y. & Sakuma, T., Role of grain boundary phase on the superplasticity deformation of tetragonal zirconia polycrystal. *J. Am. Ceram. Soc.*, **73**(10) (1990) 3069–3073.
12. Shi, J. L., Gao, J. H., Ruan, M. L. & Lu, Z. L., Compressive deformation behavior of Y-TZP-based ceramics. II, Micro-indentation toughness of compressive deformed Y-TZP and Y-TZP/Al₂O₃ composites. The following paper.
13. Shi, J. L., Zhu, G. Q., Li, L., Lu, Z. L. & Lai, T. R., Bi-axial stretching of superplastic Y-TZP and Y-TZP/Al₂O₃ ceramics in air atmosphere, to be published.

14. Shi, J. L., Lin, Z. X., Qian, W. J. & Yen, T. S., Characterization of agglomerate strength of coprecipitated superfine zirconia powders. *J. Europ. Ceram. Soc.*, **13**(3) (1994) 267–276.
15. Shi, J. L., Lin, Z. X. & Yen, T. S., Effect of agglomerates in superfine zirconia powders on compacts on the microstructural development. *J. Mater. Sci.*, **28**(2) (1993) 342–348.
16. Wakai, F. & Kato, H., Superplasticity of TZP/ Al_2O_3 composites. *Adv. Ceram. Mater.*, **3**(1) (1988) 71–76.
17. Wakai, F., Kato, H., Sakaguchi, S. & Murayama, N., Compressive deformation of Y_2O_3 -stabilized $\text{ZrO}_2/\text{Al}_2\text{O}_3$ composite. *J. Jpn Ceram. Soc.*, **94** (1986) 1017.
18. Nieh, T. G., McNally, C. M. & Wadsworth, J., Superplasticity behavior of a 20% Al_2O_3 /YTZ ceramic composite. *Scripta Met.*, **23** (1989) 457.
19. Nieh, T. G., McNally, C. M. & Wadsworth, J., Superplastic properties of a fine-grained yttria-stabilized tetragonal polycrystal of zirconia. *Scripta Metall.*, **22** (1988) 1297.
20. Ashby, M. F. & Verall, R. A., Diffusion accommodated flow and superplasticity. *Acta Metall.*, **21** (1973) 149–163.